PAPER IN FOREFRONT

CrossMark

Ion concentration in micro and nanoscale electrospray emitters

Elizabeth M. Yuill[1] · Lane A. Baker[1]

Abstract
Solution-phase ion transport during electrospray has been characterized for nanopipettes, or glass capillaries pulled to nanoscale tip dimensions, and micron-sized electrospray ionization emitters. Direct visualization of charged fluorophores during the electrospray process is used to evaluate impacts of emitter size, ionic strength, analyte size, and pressure-driven flow on heterogeneous ion transport during electrospray. Mass spectrometric measurements of positively- and negatively-charged proteins were taken for micron-sized and nanopipette emitters under low ionic strength conditions to further illustrate a discrepancy in solution-driven transport of charged analytes. A fundamental understanding of analyte electromigration during electrospray, which is not always considered, is expected to provide control over selective analyte depletion and enrichment, and can be harnessed for sample cleanup.

Keywords Microfluidics / Microfabrication · Nanoparticles / Nanotechnology · Electroanalytical methods

Introduction

The impact of "omics"-related fields [1–3], has rightfully earned mass spectrometry high acclaim. However, aspects of quantitative analysis with MS remain challenging. For instance, proteomics studies are generally biased toward analysis of proteins with high sample abundance, and some analytes may not be measured at all due to ion suppression, neutral charge state, or size-incompatibility with the chosen detector [4]. Further, tendency of the ionization technique to enhance or deplete one analyte over others can lead to results that do not reflect true sample distribution. Electrospray ionization (ESI) processes, such as Taylor cone formation [5], droplet size distribution [6], and analyte ionization [7–10], that occur after sample leaves an ESI emitter have attracted significant attention. Additional considerations prior to these events, namely, migration of ions preceding and during ionization, are also present and play a significant role in ESI when emitter

tip size is reduced to nanoscale dimensions. Migration effects in nanoscale ESI emitters provide an intriguing opportunity to either avoid or exploit quantification bias that may exist.

Electrospray ionization has been likened to a two-electrode electrochemical cell [11–14], and undergoes heterogeneous solvent changes due to electrolysis during operation. Well-studied examples of heterogeneity during ESI include buildup of potential gradients [15–17], change in pH due to proton production in positive-ionization mode [18, 19], and analyte electromigration [20–22]. Although detrimental to quantitation, heterogeneity within the emitter can be advantageous. For instance, electromigration during electrospray can be used to separate analytes, or to clean up samples in complex matrices [21–23]. Electromigration can be induced with a step-voltage, where high positive potential is used to separate matrix from analyte, followed by a step to lower positive potential during which electrosprayed sample is analyzed [22], although a recent study [21] suggests polarity-reversal is a better mode for signal enhancement and analyte separation.

In polarity-reversing high-voltage nanoelectrospray ionization (PR-nESI), a short duration of high negative potential is applied to an electrode in contact with the sample, followed by a switch to positive potentials, under which analyte signals are collected. In principle, for positively-charged large molecules (e.g. protein standards), negative applied potentials attract both analyte molecules and Na^+ toward the working electrode, which induces migration away from the emitter tip. Larger

✉ Lane A. Baker
lanbaker@indiana.edu

[1] Department of Chemistry, Indiana University, 800 E. Kirkwood Avenue, Bloomington, Indiana 47405, USA

molecules with lower mobility travel more slowly away from the emitter tip than small salt cations. Upon switching back to positive applied potentials, initial spectra show decreased salt adduction, due to this separation. Conversely, for negatively-charged large molecules, analytes can be enriched at the emitter tip under negative applied potentials, while Na^+ migrates away from the tip to effectively desalt analytes when ESI polarity is reversed [21].

Benefits to nanoESI have also been realized through use of tips with smaller openings, and include enhanced S/N ratios [24] and increased salt tolerance [25]. As popularity of small ESI emitters increases, however, researchers need to be aware of the differences that come with working at the nanoscale. For instance, as the electrical double layer (EDL) thickness approaches the size of the tip opening, ion transport deviates from macroscale behavior. These phenomena are embodied through ion current rectification and concentration polarization [26–29]. Such EDL effects are highly dependent on electrolyte concentration, which brings special consideration to nanoESI emitters that might be employed for ESI in native state [30, 31] or low salt conditions. Although ion concentration polarization has been investigated for small electrospray emitters [32], and electromigration effects have been characterized for nanoESI [20–22], these studies have relied solely on interpretation of mass spectrometry results to explain observations of heterogeneity during electrospray ionization.

In this manuscript, fluorescence microscopy of charged, fluorescent analytes is employed to directly probe solution-phase ion transport under electrospray conditions. Variables such as emitter size, solution ionic strength, and pressure-driven flow are investigated and contributions to electromigration from high electric fields or concentration polarization are reported. Knowledge of experimental parameters is especially critical for understanding sample and technique limitations, to either exploit or curtail heterogeneity within electrospray ionization.

Experimental section

Chemicals/materials

Solutions with different concentrations of potassium chloride (VWR, Radnor, PA) were prepared with 18 M$\Omega\cdot$cm H_2O from a Milli-Q water purification system (EMD Millipore, Billerica, MA). Adjustment of pH was performed through addition of hydrochloric acid (EMD Millipore, Billerica, MA) or sodium hydroxide (Mallinckrodt Chemicals, St. Louis, MO). Solutions were passed through 0.22 μm PTFE filters (Fisher Scientific, Pittsburgh, PA). Sulforhodamine B and fluorescein sodium salt were purchased from Sigma-Aldrich (St. Louis, MO) and used as received. Rhodamine B (0.2% in isopropyl alcohol, Sigma-Aldrich) was dried under

nitrogen gas, then reconstituted in a KCl solution. Sulfate beads were obtained from Thermo Fisher Scientific (Fluospheres™, 0.02 μm, yellow-green fluorescent (505/515 nm), Waltham, MA). Lysozyme and ubiquitin were obtained from Sigma-Aldrich for mass spectrometry experiments.

Nanopipette fabrication/characterization

Quartz capillaries (Q100-70-7.5, Sutter Instruments, Novato, CA) with 1.0 mm outer diameter (o.d.) and 0.7 mm inner diameter (i.d.) were pulled with a laser-based pipette puller (Sutter Instrument) to tip diameters from 60 to 140 nm. All capillaries were piranha cleaned prior to pulling. *(CAUTION: "piranha" solution reacts violently with organic materials and must be handled with extreme care.)* New Objective PicoTips (BG-10-58-2-N-20) were obtained from Scientific Instrument Services, Inc. (Ringoes, NJ) and consisted of uncoated borosilicate glass with 1.0 mm o.d. and 0.58 mm i.d. PicoTips were used as received. Emitters were characterized with electron microscopy (scanning electron microscopy, SEM, and scanning transmission electron microscopy, STEM) before and after experiments (Quanta FEG 600F, FEI, Hillsboro, OR).

Both emitter types (nanopipettes and micron-sized PicoTips) were backfilled through use of a MicroFil needle (World Precision Instruments, Sarasota, FL). For solutions that contained small molecules, centrifugation was used to drive fluid to the nanopipette tip. Centrifugation of FluoSpheres™, however, often resulted in a cluster of particles at the nanopipette tip, thus nanopipettes filled with FluoSpheres™ were subjected to a 100 psi back-pressure for 2-10 minutes until the tips were wetted, as determined by optical microscopy. PicoTips were backfilled only; no additional steps were required to wet the tip, as the PicoTips had a filament throughout the capillary body.

Instrumental setup

To monitor fluorescence during electrospray, emitters were filled with fluorescent solutions and laid side-on under the objective of a Nikon Eclipse microscope (E800, Nikon Instruments, Melville, NY), equipped with a mercury lamp (Model HB-10101AF, Nikon) and FITC and TRITC filters. A Pt wire (0.127 mm, Alfa Aesar, Ward Hill, MA) was back-inserted into the pipette for potential application from a 500 V power supply (PMC500-0.1A, Kikusui, Santa Clara, CA) and the resultant current to a floating stainless steel coupon was measured via a Keithley 410A (Keithley Instruments, Cleveland, OH). For larger (micron-sized) emitters, a high voltage power supply (Electrospray Control Unit, Fisons Instruments, Ipswich, United Kingdom) was employed. Images were acquired with QCapture Pro 6.0 (QImaging, Surrey, BC, Canada) software.

Most experiments were performed with self-aspirated flow, however, a syringe pump (NE-1600, New Era Pump Systems, Inc., Farmingdale, NY) was used to conduct pressure-driven flow experiments for comparison of fluorophore movement. For this setup, pipettes were connected to a Hamilton gastight syringe pump (#1750, Hamilton Company, Reno, NV) through a segment of PE tubing and a union (dual small hub RN coupler, Hamilton Company). Potential was applied to a stainless steel segment of tubing ca. 6" in length.

Mass spectrometry experiments were performed on a Bruker Daltonics micrOTOF (Billerica, MA) in positive ion mode at 190°C. Emitters were positioned 1-2 mm away from the capillary inlet. Spectra were acquired from m/z 500 – 2500 at a rate of 1 Hz. After 0.2 minutes, a potential of +1.2 kV or +1.8 kV was applied to nanopipette or micronsized emitters, respectively, by biasing the mass spectrometer inlet at negative potential and holding the pipette electrode at ground. Potential was held constant over a 10 minute period, or until spray had stopped, as determined by a drop in total ion current intensity. Prior to analysis, the instrument was calibrated with 20 mM sodium trifluoroacetate (Sigma-Aldrich) in a 50:50 methanol:acetonitrile solution.

Data analysis

Images were processed with ImageJ (National Institutes of Health, Bethesda, MD). Line scans of fluorescence intensity were taken axially across a pipette body over several frames of a movie. Fluorescence of an area off the pipette was also measured to obtain a blank value. Fluorescence intensities were recorded if values exceeded three times the blank value, otherwise a zero value was input. Next, a matrix of fluorescence intensities across distance for all frames of the movie was compiled. The maximum value from the matrix was determined and all values were normalized against the maximum fluorescence intensity.

To determine distance of the fluorescence signal from the pipette tip, an arbitrary threshold of 15% maximum fluorescence was chosen, such that the distance at which fluorescence values met or exceeded 15% was recorded as the "distance from the tip" (vide infra, Figures 2 and 3).

Results and discussion

Small molecule electromigration

Migration of fluorophores during electrospray was initially performed with small molecules. For a given ion in a low ionic strength solution (e.g. 500 μM KCl) and at neutral pH, movement due to electromigration results from both electroosmotic flow (EOF) and electrophoretic migration. EOF for an emitter with a negatively-charged wall will occur from anode to cathode, viz., toward the emitter tip for positive applied potentials and away from the emitter tip at negative applied potentials. Electrophoretic migration for anions will oppose EOF, while cations will migrate in the same direction as EOF. If electrophoretic forces are sufficiently large relative to EOF, anion migration toward the emitter tip will occur under negative potential application, and migration away from the emitter tip will occur under positive potential application, while cations will migrate in an opposite fashion; away from the emitter tip during negative potential application and toward the emitter tip during positive potential application. For a given system with an anionic fluorophore and non-fluorescent supporting electrolyte, fluorescence microscopy would result in observed enrichment or depletion in fluorescence at the emitter tip, for negative or positive applied potentials, respectively, depicted theoretically in Figure 1a and b. Cations and anions in supporting electrolyte are effectively invisible.

Fluorescence of sulforhodamine B was monitored during electrospray at both positive and negative polarities. Sulforhodamine B was chosen due the anionic nature of the analyte across a broad pH range (2–12) [33]. In Figure 1c, a solution of 200 μM sulforhodamine B with 500 μM KCl (unbuffered, at pH = 7.0), was filled in an ~80 nm pipette and subjected to a positive potential of magnitude large enough to induce electrospray, as monitored by electrospray current. Gradual depletion of fluorescence from the emitter tip was observed, with the majority of fluorescence signal migrating ~500 μm from the emitter tip after ~80 s. The polarity applied was then switched and fluorescence was again monitored over time. Migration of sulforhodamine B toward the emitter tip occurred, and after ~80 s, fluorescent signal was distributed evenly throughout the emitter, as shown prior to the application of potential. If the order of experiments was reversed, and positive potentials were applied initially, enrichment of sulforhodamine B at the emitter tip was observed, however such high local concentrations were typically accompanied by a large spike in current, after which the emitter tip was broken (data not shown).

Sulforhodamine B results indicated electrophoretic mobility was markedly higher than EOF under employed conditions. To understand EOF contributions toward electromigration during electrospray, rhodamine B, a zwitterion at neutral pH that has been used as a marker for electroosmotic flow [34], was tested. These control studies, shown in the Electronic Supplementary Material (ESM) in Fig. S1 for 200 μM rhodamine B with 500 μM KCl (unbuffered, at pH = 7.0), demonstrated no observable movement of fluorescence signal under either positive or negative polarity over ~200 s, which confirms expectations that EOF may not be a key driving force during electrospray at these conditions.

To understand how emitter surface charge influenced both EOF and ion transport due to confinement within a narrow tip

Fig. 1 Schematic of (a) depletion and (b) enrichment of a negatively-charged analyte under positive and negative applied potentials, respectively. Analyte is represented by a red circle, while supporting electrolyte cation and anion movement are indicated by yellow and blue circles, respectively. Fluorescence images of sulforhodamine B (200 μM with 500 μM KCl, pH = 7.0) under (c) +500 V applied potential (V_{app}) and (d) -500 V_{app} at t = 1.97 s, 39.40 s, and 78.80 s after potential was turned on. Note: +V_{app} experiment in (c) was conducted immediately prior to application of -V_{app} in (d)
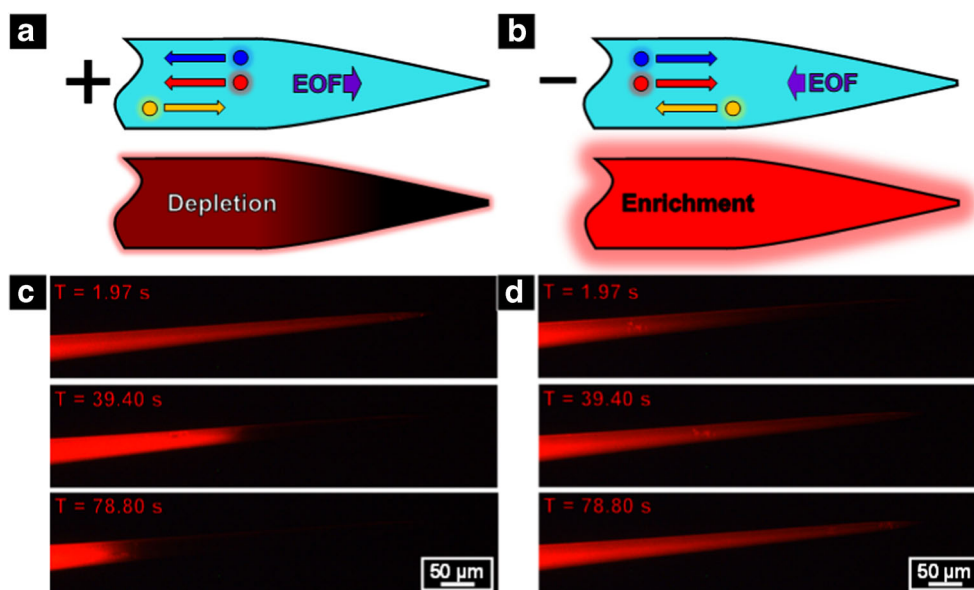
opening, attempts were made to silanize the inner pipette walls, to render the quartz surface positively-charged. Characterization of the tip after silanization was performed by filling the pipette with a conductive solution and immersing the pipette in a bath of the same solution. A potential sweep from -1 V to +1 V was applied between a Ag/AgCl working electrode in the pipette and a Ag/AgCl reference electrode in bath solution and the resultant current was monitored with a Keithley picoammeter/voltage source (Keithley 6487, Keithley Instruments). Ion current for bare quartz pipettes rectifies in the negative direction, viz., the magnitude of current that passes under positive applied potential is attenuated relative to the current magnitude at the same potential but with negative polarity. After pipette silanization, positive rectification was observed, which indicated that the pipette walls were successfully functionalized. However, these attempts at reversing the surface charge with silanes were unstable, as after fluorescence experiments under sufficient potential to induce electrospray, current–voltage (I–V) curves (measured in solution, as described above) showed characteristic negative rectification, which indicated that after subjecting the modified pipettes to high electric fields, surface charge was negative, as with un-modified pipettes.

While alteration of surface charge through covalent modification is more ideal, pipette surface charge can also be altered by subjecting the quartz walls to sufficiently acidic conditions. Fig. S2 (see ESM) shows a solution of sulforhodamine B with 500 μM KCl at pH = 1.5. At this low pH, silanol groups are protonated and of neutral charge, so migration due to EOF should be zero. In ESM Fig. S2, no movement of sulforhodamine B was observed under either polarity, as expected. One caveat, however, is that the decreased solution pH is accompanied by an increase in overall solution conductivity, as result of pH adjustment with acid. Increased conductivity, or

ionic strength, causes screening of charges at the glass wall, which decreases concentration polarization (discussed further vide infra). Additionally, at pH = 1.5, a subpopulation of sulforhodamine B may protonate, causing neutralization of anionic analyte.

To further explore impact of pH on analyte movement, solutions of fluorescein were tested. Fluorescein (200 μM) in an unbuffered aqueous solution (500 μM KCl, starting pH = 7.0) demonstrated depletion for low positive potentials (e.g. +300 V, with currents < 3 nA), enrichment for high positive potentials (e.g. +500 V, with currents > 3nA) and depletion for negative applied potentials (shown in ESM Fig. S3). While depletion at low positive potentials is similar behavior to previously-tested anionic fluorophore, sulforhodamine B, enrichment of anions at higher magnitude of positive potential opposed theory. One likelihood is that solution pH changes become significant throughout the experiment, enough to protonate and neutralize, or even make cationic, fluorescein. Under conditions employed (low ionic strength, unbuffered pH), protons are generated due to water electrolysis from the electrospray process [19] and the rate of electrolysis is higher for greater positive applied potentials. Since experiments are performed sequentially (first low positive potentials, then high positive potentials, then negative potentials), solutions at high positive potential likely become sufficiently acidic to protonate fluorescein [35], which changes the charge from anionic to cationic. At higher positive applied potentials, enrichment of the now cationic species should occur, and subsequent negative applied potential would result in depletion at the emitter tip, as observed. To test this, the same concentration of fluorescein in 10 mM phosphate buffer at pH = 7.0 was employed. In general, fluorescein under buffered conditions behaved as expected for anionic species (enrichment under positive applied potentials and depletion under negative applied

potentials was observed). However, under negative potential application, the concentrated fluorescein localized at the pipette tip was observed to precipitate from solution, along with a corresponding spike in current, which broke the pipette tips. Subsequent studies of fluorescein were performed only at low positive potentials, to maintain fluorescein in an anionic state and also to avoid increasing local concentration too high, as resulted from negative potential application.

Impact of emitter size on electromigration

Micron-sized emitters were filled with solutions that contained small molecule fluorophores to observe whether electromigration effects were size-dependent. Both micron-sized emitters (New Objective PicoTips, measuring ~3-4 μm) and nanoscale emitters (60-80 nm i.d.) were filled with the same solution of 200 μM sulforhodamine B with 500 μM KCl (unbuffered, at pH = 7.0). Application of a positive potential caused rapid depletion of fluorescence away from the emitter tip for the nanopipettes, whereas no noticeable electromigration was observed for the micron-sized emitters, as shown in Figure 2. Migration of fluorescence signal could be quantitated by measuring a line scan of fluorescence across the emitter body axially (shown in Figure 2a and b brightfield images). Fluorescence intensities were acquired for each frame of a movie, and were normalized to the maximum fluorescence intensity across all acquired frames, for a given emitter. Note: fluorescence values higher than 3× an average fluorescent intensity off the pipette body were kept, while intensities below this threshold were assigned

a zero value. Distribution of fluorescence signal across the pipette body over time shows that for nanoscale emitters, rapid depletion of anionic fluorophore occurs under positive applied potentials, with depletion almost to the edge of the acquired frame within ~90 s (Figure 2e). For micron-sized emitters, however, there is minimal change over a period of 200 s (Figure 2f). A frame-by-frame comparison over a range from 2 s to 90 s after initial potential application is shown in Fig. S4.

Similarly, solutions of fluorescein (200 μM in 500 μM KCl, unbuffered at pH = 7.1) demonstrated rapid depletion for nanoscale emitters and minimal change for micron-sized emitters under positive potentials (Fig. S5). Differences in analyte electromigration for different sized emitters may stem from two effects: (i) electric field differences between micro- and nanoscale emitters and (ii) contributions of the electrical double layer to alter ion transport at the emitter tips. Previous reports have shown that small electrospray emitters support much higher electric fields, which are localized at the highest aspect ratio of the emitter tip [24]. Herein, both emitter sizes were evaluated at a constant distance (ca. ~1 mm) between the emitter and floating, conductive plate, from which current was measured. Potential was ramped until a stable spray was achieved, as indicated by a non-fluctuating electrospray current. Thus, for the same distance between the emitter and plate, electric fields (E_s) were nearly an order of magnitude larger for the nanopipette versus the micron-sized emitter (1.26×10^8 V/m for the 2.87 μm emitter vs. 1.64×10^9 V/m for the 80 nm emitter for sulforhodamine B, and 9.53×10^7 V/m for the 3.64 μm
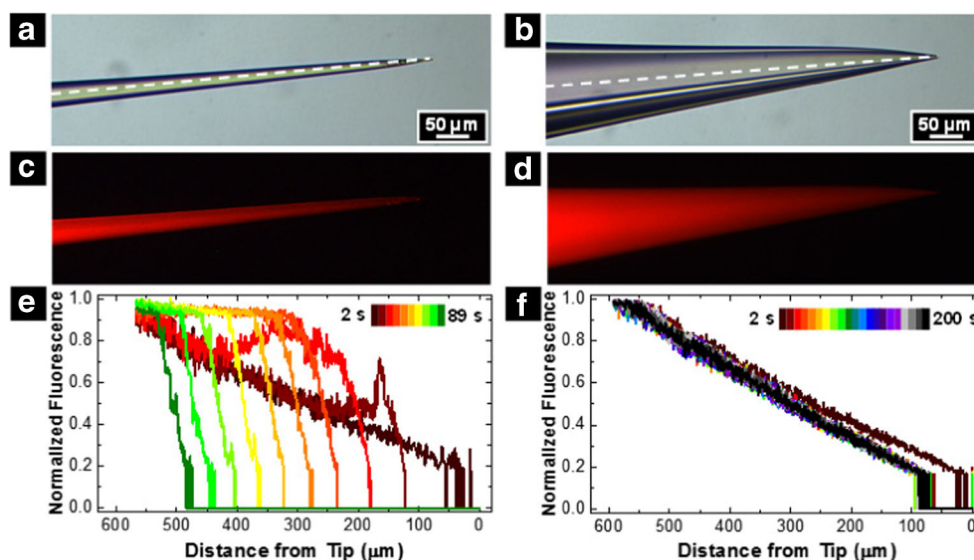

Fig. 2 Bright field images of (a) nanopipette (inner diameter, i.d. = 83 nm) and (b) PicoTip (i.d. = 2.87 μm) prior to electrospray of 200 μM sulforhodamine B with 500 μM KCl, pH = 7.0. Applied potential was +504 V and +960 V for nanopipette and PicoTip, respectively. Corresponding fluorescence images of (c) nanopipette and (d) PicoTip.

Line scans (e and f, for nanopipette and PicoTip, respectively) show normalized fluorescence intensity versus distance from the emitter tip over time. Line scans were taken axially through the pipette body, depicted by the dotted lines in (a) and (b)

emitter vs. 7.69×10^8 V/m for the 104 nm emitter for fluorescein, as determined from the analytical equation, Eq. 1 [36].

$$E = \frac{AV}{r\ln(4d/r)} \tag{1}$$

where A is an empirically-derived constant of 1.499 [37, 38], V is potential between the emitter tip and floating, conductive plate, r is the emitter radius, and d is distance between the emitter tip and floating, conductive plate.

Second, for small emitter size, the electrical double layer thickness occupies a greater percent of the cross sectional area, which, for a negatively-charged wall surface, hinders anion transport through the tip opening (discussed more vide infra). For instance, EDL thickness, δ, for a 500 μM monovalent 1:1 electrolyte at 298 K is ~14 nm. For a 100 nm i.d. tip, the EDL would occupy ~50% of the cross sectional tip opening, whereas for a 3 μm tip, only ~2% of the tip opening would be occupied by the EDL. Hence, heterogeneity of ion transport at the tip is of greater impact for emitters with small tip size.

Influence of ionic strength on electromigration/concentration polarization

EDL thickness decreases with increased ionic strength, due to charge screening by ions in solution. Thus, contributions to hindered anion transport should be decreased for high ionic strength solutions. For low ionic strength solutions and nanoscale pores, EDL overlap can occur, although complete overlap is not necessary for significant changes to occur in ion transport. In literature, concentration polarization and ion current rectification have been investigated experimentally [26–29]. Fluorescein movement can be used to understand concentration polarization for nanoscale emitters filled with low ionic strength solution. When a pipette filled with an electrolyte solution that contained fluorescein was immersed in a bath solution and potential was scanned between an electrode in the pipette and a reference electrode in the bath solution, ion current and fluorescence microscopy illustrated altered ion transport under positive and negative polarities [29]. Both enrichment of fluorescence in the nanopipette tip and enhancement of ion current were observed under negative potential application, while fluorescence depletion and attenuation of ion current were observed for positive applied potentials. These effects, namely, the asymmetry between ion current at different polarities with the same magnitude of potential (i.e. ion current rectification), and local concentration polarization of the anionic fluorophore, have been attributed to a discrepancy between anion/cation transport at the nanoscale when EDL thickness is significant, relative to ion transport in bulk solution [26]. Similarly, when solutions of fluorescein with higher supporting electrolyte concentration were

tested under the same setup, ion currents were not rectified (current magnitudes at positive and negative polarities were the same), and no depletion or enrichment of fluorescein was observed. These studies were expanded to our electrospray setup, to determine what impact ionic strength has on electromigration of analytes during electrospray.

Due to complexities surrounding small molecules (i.e. pH-dependent charge, described vide supra), highly-charged, fluorescent nanoparticles, FluoSpheres™, were employed for the remaining studies. The 20 nm particles have sulfate surface groups, which provide a negative charge at neutral pH. A solution of 0.94 μM Fluospheres™ with either 500 μM (low ionic strength) or 50,000 μM (50 mM, high ionic strength) KCl (unbuffered, at pH = 7.0) were backfilled into nanoscale emitters and observed with fluorescence microscopy under positive bias. For both solutions, depletion of the anionic particles occurred. However, depletion for the lower ionic strength solution (500 μM KCl) occurred much more rapidly, as shown in the frame-by-frame comparison in Fig. S6 (see ESM).
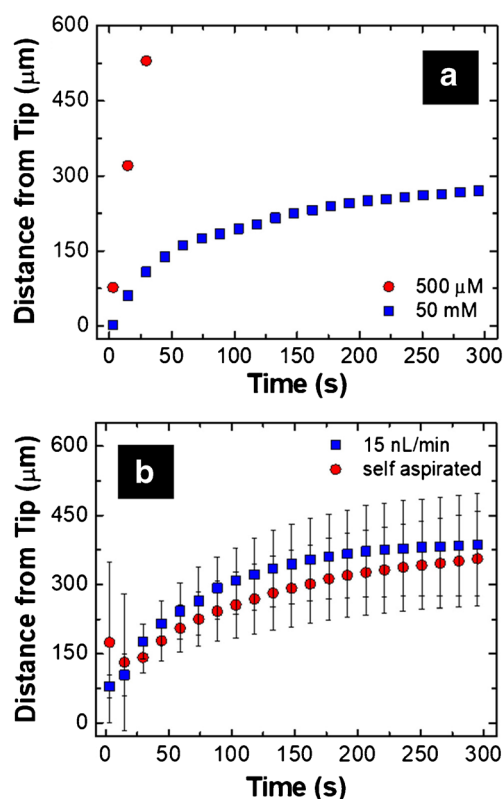

Fig. 3 (a) Ionic strength influence. Depletion of negatively-charged sulfate-Fluospheres™ (0.94 μM) under $+V_{app}$ occurs faster for a 500 μM KCl vs. a 50,000 μM KCl solution. Pipette sizes shown here were 95 nm i.d. and 77 nm i.d. for the 500 μM and 50 mM ionic strength data sets, respectively. (b) Depletion of negatively-charged sulfate-Fluospheres™ (0.94 μM with 50 mM KCl, pH = 7.1) under $+V_{app}$ for self-aspirated (n = 10, pipette size: 98 ± 19 nm i.d) and pressure-driven (n = 5, pipette size: 121 ± 14 nm i.d.) electrospray. A syringe pump flow rate of 15 nL/min was used for pressure-driven flow

Fluorescence depletion could be quantified over time by taking line scans axially across the pipette body. When fluorescence signal met or exceeded an arbitrarily-chosen threshold of 15% maximum fluorescence, the distance from the pipette tip was recorded. This distance was acquired across all frames and plotted as a function of time. The resultant plots (in Figure 3a) show the dramatic difference in fluorescence depletion for the solutions with high and low ionic strengths; full depletion (>520 μm from the pipette tip) was observed within 30 s for the low ionic strength solution, while depletion had only reached ~270 μm from the pipette tip at 300 s for the high ionic strength solution. Pipettes remained intact throughout experiments, as demonstrated via comparison of scanning transmission electron microscopy images prior to and after experiments (ESM Fig. S7).

Electromigration under pressure-driven flow

In practice, nanoESI emitters are commonly coupled to a syringe pump for pressure-driven flow. For an anion under positive potentials, pressure-driven flow would oppose electrophoretic movement in solution. To understand whether contributions from pressure-driven flow would overcome electromigration away from the emitter tip, a comparison between self-aspirated and pressure-driven conditions was performed for nanopipettes filled with a solution of 0.94 μM FluoSpheres™ with 50 mM KCl (unbuffered, at pH = 7.1). NanoESI emitters of ~100 nm have only recently gained

popularity, hence, optimization of pressure-driven flow has not been reported in literature. A flow rate of 15 nL/min was chosen, scaled-down from a survey of literature for common flow rates used with larger emitters. Pipettes were equilibrated for one minute after initiation of pressure-driven flow from the syringe pump and prior to potential application. A comparison of fluorescence depletion over time for 10 self-aspirated pipettes to 5 pressure-driven flow pipettes is shown in Figure 3b. While error bars are large, due to pipette-to-pipette variation, there was no significant difference between pipettes electrospraying via means of self-aspiration or pressure-driven flow. At high enough flow rates, one would expect net movement of solution toward the tip would overcome depletion of anions, however such high flow rates may prove detrimental to tip survival after experiments.

Emitter size dependence for mass spectrometric acquisition of proteins

To further demonstrate the impact small emitters have on analyte selectivity during electrospray, mass spectrometric experiments on positively- and negatively-charged proteins were performed. Solution that contained 10 μM lysozyme, 10 μM ubiquitin and 500 μM KCl at pH = 7.5 was loaded into nanopipette and micron-sized emitters. Due to the isoelectric points of lysozyme (11.3) [39] and ubiquitin, (6.7) [39], lysozyme should be cationic and ubiquitin should be anionic under employed conditions.

Fig. 4 Mass spectra of 10 μM lysozyme, 10 μM ubiquitin, 500 μM KCl at pH = 7.5 from a nanopipette (a, b) and micron-sized emitter (c, d). Potentials were applied and held constant. Mass spectra represent an 8-scan average at (a) 0 min and (b) 5 min after a +1.2 kV potential was applied to a 109 nm i.d. emitter and at (c) 0 min and (d) 2.5 min after a +1.8 kV potential was applied to a 5.9 μm o.d. emitter. Peak assignments are in red for lysozyme and blue for ubiquitin
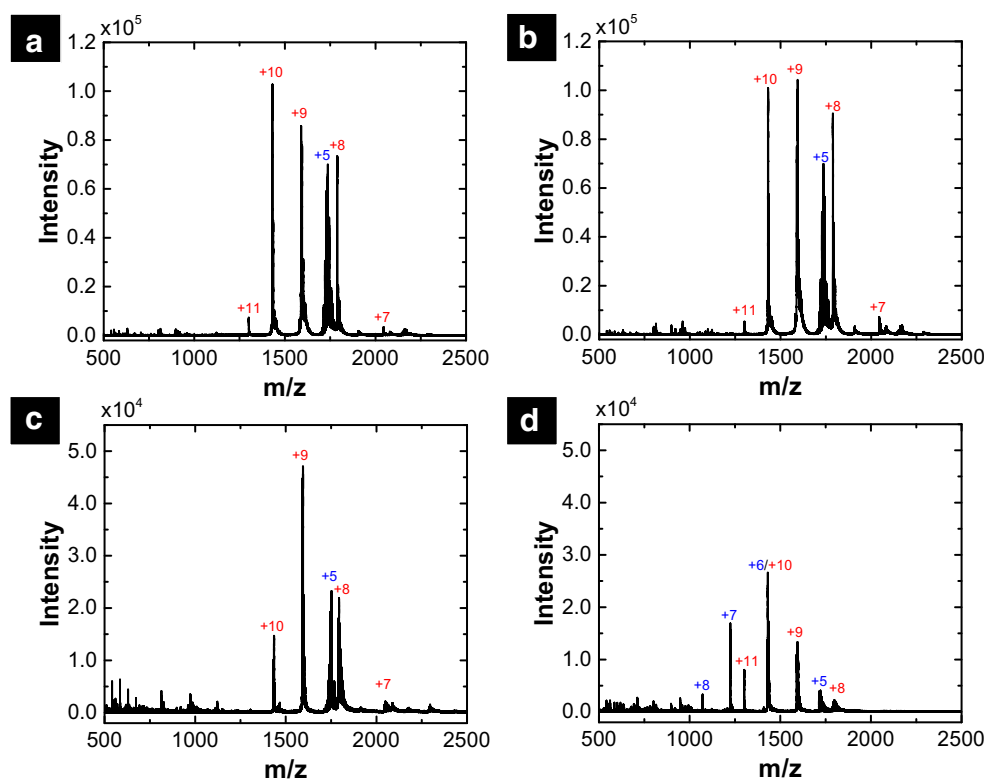
Fig. 5 Total ion chromatogram (TIC) and extracted ion chromatograms (EICs) for 10 µM lysozyme, 10 µM ubiquitin, 500 µM KCl at pH = 7.5 sprayed from a (a) 109 nm i.d. nanopipette and a (b) 5.9 µm o.d. emitter. Potential of +1.2 kV or +1.8 kV (for nanopipette and micron-sized emitter, respectively) was applied at 0.2 minutes and held constant for 10 minutes, or until spray had stopped. EIC signal was collected from the lysozyme +9 peak (at m/z = 1590) and the ubiquitin +7 peak (at m/z = 1224)
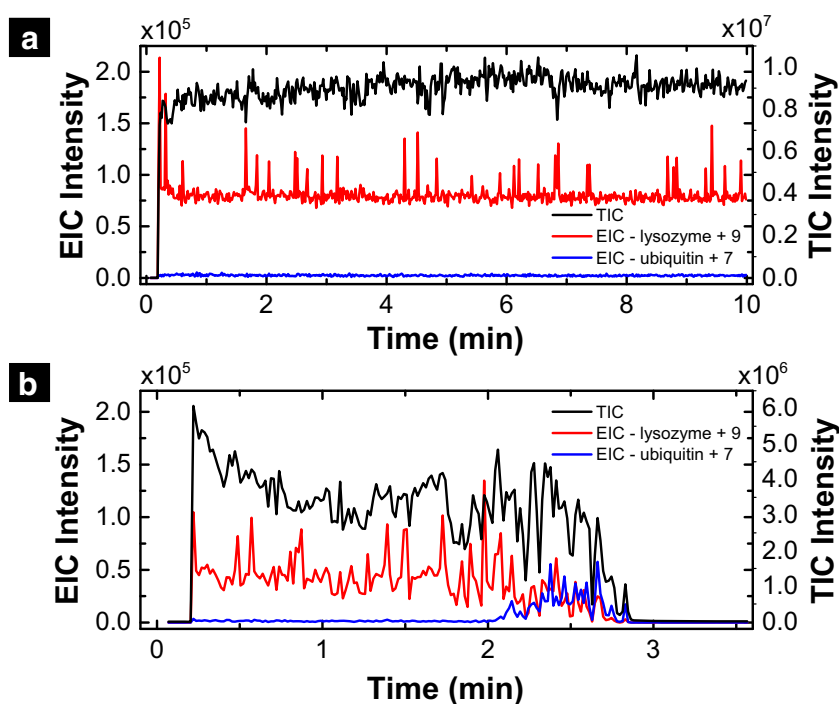
Thus, under a positive applied potential, we expect lysozyme should migrate toward the emitter tip and ubiquitin should migrate away from the emitter tip (toward the working electrode). A +1.2 kV or +1.8 kV potential (to the nanopipette or micron-sized emitter, respectively) was applied 0.2 minutes into data acquisition and the potential was held constant for 10 minutes, or until loss of spray, as determined by drop in total ion current.

Representative mass spectra, and total and extracted ion chromatograms are shown in Figures 4 and 5. Initially, at t = 0 min after potential application, both emitter sizes show a distribution of lysozyme peaks (from +7 to +11 for the nanopipette, and from +7 to +10 for the micron-sized emitter) and a ubiquitin +5 peak with extensive alkali-adduction, shown in more detail in ESM Fig. S8 (Figure 4a and c). Replicate measurements for micro and nanoscale emitters can also be found in ESM Fig. S9 (microscale) and ESM Fig. S10 (nanoscale). Spray from the nanopipette emitters (n = 6) was stable over >10 minutes, as seen in the total ion current and extracted ion current for lysozyme +9 at m/z = 1590 (Figure 5a). Moreover, peak distributions were unchanged over that time period. A mass spectrum averaged over eight scans (Figure 4b) at 5 minutes after potential application shows spectra consistent with t = 0 minutes. In contrast, spray from micron-sized emitters (n = 5) had higher variation in total ion chromatogram, with a complete loss of signal well before 10 minutes. In Figure 5b, for instance, signal intensity drops to zero at ~2.6 minutes after potential application.

Just before loss in signal, intensity for higher charge states of ubiquitin increases, as seen in the extracted ion chromatogram

of ubiquitin +7 at m/z = 1224 (Figure 5b). An averaged mass spectrum, taken at 2.5 minutes after potential application, in Figure 4d, shows a wider distribution of charges on ubiquitin than at t = 0 min, with peaks from +5 to +8 charge states present. This shift at ~1.9 minutes after potential application may correspond to electroosmotic forces overcoming electrophoretic forces that drive the negatively-charged ubiquitin away from the tip. Contrastingly, nanopipette electrospray of the same solution over a longer time period (>10 minutes) does not show an increase in peak intensity for the high charge state ubiquitin, which indicates that electrophoretic forces in the small emitters may be higher than for the micron-sized emitters. While both emitter types demonstrate differences between positive and negative analyte electrospray at low ionic strength, nanopipettes completely suppress the ubiquitin signal via depletion away from the emitter tip over the 10 minute period investigated.

Conclusions

Analyte migration during electrospray has been characterized via fluorescence microscopy and mass spectrometry for nanoscale emitters. Contributions both from high electric field at the nanoscale emitters and from the concentration polarization phenomenon make nanoscale emitters especially susceptible to heterogeneous analyte distribution within the emitter tip, relative to microscale emitters. These effects are pronounced at low ionic strength, which is especially pertinent for native mass spectrometry investigations, and occur for both small

molecules and particles in solution. Understanding which factors contribute to, and exacerbate, heterogeneity of solution-phase ion transport during electrospray is critical for control of experimental outcome. For instance, high ionic strengths or larger emitters may be necessary to reduce heterogeneity for semi-quantitative experiments, such as direct sampling and subsequent ESI of biological species [40]. In contrast, heterogeneity may be exploited for sample cleanup or signal enhancement purposes [20–22]. In either case, a fundamental understanding of experimental variables is integral to performing informed research.

Compliance with ethical standards

This study required no human or animal samples and research conducted complied with ethical standards set forward by Indiana University.

Conflict of interest The authors declare that they have no competing interests.

References

1. Aebersold R, Mann M. Mass spectrometry-based proteomics. Nature. 2003;422:198–207.
2. Yates JR, Ruse CI, Nakorchevsky A. Proteomics by mass spectrometry: approaches, advances, and applications. Annu Rev Biomed Eng. 2009;11:49–79.
3. Dettmer K, Aronov PA, Hammock BD. Mass spectrometry-based metabolomics. Mass Spectrom Rev. 2007;26:51–78.
4. Bantscheff M, Schirle M, Sweetman G, Rick J, Kuster B. Quantitative mass spectrometry in proteomics: a critical review. Anal Bioanal Chem. 2007;389:1017–31.
5. Marginean I, Parvin L, Heffernan L, Vertes A. Flexing the electrified meniscus: the birth of a jet in electrosprays. Anal Chem. 2004;76:4202–7.
6. Gomez A, Tang K. Charge and fission of droplets in electrostatic sprays. Phys Fluids. 1994;6:404–14.
7. Dole M, Mack LL, Hines RL, Mobley RC, Ferguson LD, Alice MB. Molecular beams of macroions. J Chem Phys. 1968;49:2240–9.
8. Iribarne JV, Thomson BA. On the evaporation of small ions from charged droplets. J Chem Phys. 1976;64:2287–94.
9. Ahadi E, Konermann L. Modeling the behavior of coarse-grained polymer chains in charged water droplets: implications for the mechanism of electrospray ionization. J Phys Chem B. 2012;116:104–12.
10. Konermann L, Rodriguez AD, Liu J. On the formation of highly charged gaseous ions from unfolded proteins by electrospray ionization. Anal Chem. 2012;84:6798–804.
11. Blades AT, Ikonomou MG, Kebarle P. Mechanism of electrospray mass spectrometry. electrospray as an electrolysis cell. Anal Chem. 1991;63:2109–14.
12. Van Berkel GJ, Zhou F. Electrospray as a controlled-current electrolytic cell: electrochemical ionization of neutral analytes for detection by electrospray mass spectrometry. Anal Chem. 1995;67:3958–64.
13. Hop CECA, Saulys DA, Gaines DF. Electrospray mass spectrometry of borane salts: the electrospray needle as an electrochemical cell. J Am Soc Mass Spectrom. 1995;6:860–5.
14. Jackson GS, Enke CG. Electrical equivalence of electrospray ionization with conducting and nonconducting needles. Anal Chem. 1999;71:3777–84.
15. Li Y, Pozniak BP, Cole RB. Mapping of potential gradients within the electrospray emitter. Anal Chem. 2003;75:6987–94.
16. Pozniak BP, Cole RB. Ambient gas influence on electrospray potential as revealed by potential mapping within the electrospray capillary. Anal Chem. 2007;79:3383–91.
17. Pozniak BP, Cole RB. Negative ion mode evolution of potential buildup and mapping of potential gradients within the electrospray emitter. J Am Soc Mass Spectrom. 2004;15:1737–47.
18. Van Berkel GJ, Zhou FM, Aronson JT. Changes in bulk solution ph caused by the inherent controlled-current electrolytic process of an electrospray ion source. Int J Mass Spectrom Ion Processes. 1997;162:55–67.
19. Van Berkel GJ, Asano KG, Schnier PD. Electrochemical processes in a wire-in-a-capillary bulk-loaded, nano-electrospray emitter. J Am Soc Mass Spectrom. 2001;12:853–62.
20. Hu J, Jiang X-X, Wang J, Guan Q-Y, Zhang P-K, Xu J-J, et al. Synchronized polarization induced electrospray: comprehensively profiling biomolecules in single cells by combining both positive-ion and negative-ion mass spectra. Anal Chem. 2016;88:7245–51.
21. Gong X, Xiong X, Zhao Y, Ye S, Fang X. Boosting the signal intensity of nanoelectrospray ionization by using a polarity-reversing high-voltage strategy. Anal Chem. 2017;89:7009–16.
22. Wei Z, Han S, Gong X, Zhao Y, Yang C, Zhang S, et al. Rapid removal of matrices from small-volume samples by step-voltage nanoelectrospray. Angew Chem Int Ed. 2013;52:11025–8.
23. Wang Q, Zhong H, Zheng Y, Zhang S, Liu X, Zhang X, et al. Analyte migration electrospray ionization for rapid analysis of complex samples with small volume using mass spectrometry. Analyst. 2014;139:5678–81.
24. Yuill EM, Sa N, Ray SJ, Hieftje GM, Baker LA. Electrospray ionization from nanopipette emitters with tip diameters of less than 100 nm. Anal Chem. 2013;85:8498–502.
25. Juraschek R, Dülcks T, Karas M. Nanoelectrospray — more than just a minimized-flow electrospray ionization source. J Am Soc Mass Spectrom. 1999;10:300–8.
26. Wei C, Bard AJ, Feldberg SW. Current rectification at quartz nanopipet electrodes. Anal Chem. 1997;69:4627–33.
27. Ai Y, Zhang M, Joo SW, Cheney MA, Qian S. Effects of electro-osmotic flow on ionic current rectification in conical nanopores. J Phys Chem C. 2010;114:3883–90.
28. Sa N, Baker LA. Experiment and simulation of ion transport through nanopipettes of well-defined conical geometry. J Electrochem Soc. 2013;160:H376–H81.
29. Shi W, Sa N, Thakar R, Baker LA. Nanopipette delivery: influence of surface charge. Analyst. 2015;140:4835–42.
30. van Duijn E, Bakkes PJ, Heeren RMA, van den Heuvel RHH, van Heerikhuizen H, van der Vies SM, et al. Monitoring macromolecular complexes involved in the chaperonin-assisted protein folding cycle by mass spectrometry. Nat Methods. 2005;2:371–6.
31. Verkerk UH, Kebarle P. Ion-ion and ion-molecule reactions at the surface of proteins produced by nanospray. Information on the number of acidic residues and control of the number of ionized acidic and basic residues. J Am Soc Mass Spectrom. 2005;16:1325–41.
32. Hu J, Guan Q-Y, Wang J, Jiang X-X, Wu Z-Q, Xia X-H, et al. Effect of nanoemitters on suppressing the formation of metal adduct ions

in electrospray ionization mass spectrometry. Anal Chem. 2017;89: 1838–45.

33. Mchedlov-Petrossyan NO, Shapovalov SA, Egorova SI, Kleshchevnikova VN, Arias Cordova E. A new application of rhodamine 200 b (sulfo rhodamine b). Dyes Pigm. 1995;28:7–18.

34. Milanova D, Chambers RD, Bahga SS, Santiago JG. Electrophoretic mobility measurements of fluorescent dyes using on-chip capillary electrophoresis. Electrophoresis. 2011;32:3286–94.

35. Martin MM, Lindqvist L. The ph dependence of fluorescein fluorescence. J Lumin. 1975;10:381–90.

36. Eyring CF, MacKeown SS, Millikan RA. Fields currents from points. Phys Rev. 1928;31:900–9.

37. Jones AR, Thong KC. The production of charged monodisperse fuel droplets by electrical dispersion. J Phys D: Appl Phys. 1971;4:1159–66.

38. Smith DPH. The electrohydrodynamic atomization of liquids. IEEE Trans Ind Appl. 1986;IA-22:527–35.

39. Hemdan ES, Zhao Y-J, Sulkowski E, Porath J. Surface topography of histidine residues: a facile probe by immobilized metal ion affinity chromatography. Proc Natl Acad Sci U S A. 1989;86:1811–5.

40. Saha-Shah A, Green CM, Abraham DH, Baker LA. Segmented flow sampling with push-pull theta pipettes. Analyst. 2016;141: 1958–65.

Lane A. Baker is presently a James F. Jackson Associate Professor of Chemistry at Indiana University. His research interests include electroanalytical chemistry, small scale sampling, and scanned probe microscopies. He is especially interested in applications of nanopipettes towards these tasks, and specifically to applications related to scanning ion conductance microscopy and small-scale sampling for mass spectrometry.

Elizabeth M. Yuill received a B.S. in chemistry from the University of Michigan in 2012. In 2017, she received her Ph.D. under the guidance of Professor Lane A. Baker at Indiana University. In the Baker group, her research focus was on fundamentals of electrospray from nanoscale emitters, as well as development of scanning electrospray microscopy. She recently joined the Chemical & Synthetic Development Department at Bristol-Myers Squibb.